The Ni-Containing Carbon Monoxide Dehydrogenase Family: Light at the End of the Tunnel?¶

Paul A. Lindahl

Contribution from the Departments of Chemistry and of Biochemistry and Biophysics

Texas A&M University, College Station, TX 77843-3255

Phone: 979-845-0956

Fax: 979-845-4719

Email: Lindahl@mail.chem.tamu.edu

¶This work was supported by the National Institutes of Health (GM46441) and the Department of Energy (DE-F603-01ER15177).

Running Title: Ni-Containing Carbon Monoxide Dehydrogenases

Abbreviations and Textual Footnotes

1. Abbreviations: $CODH_{Gs}$, monofunctional carbon monoxide dehydrogenases, with superscript Gs indicating the genus and species of the organism from which the enzyme was isolated; $ACS/CODH_{Gs}$, bifunctional enzymes that catalyze the synthesis and/or degradation of acetyl-Coenzyme A as well as the reversible reduction of CO_2 to CO. CoFeSP, the corrinoid-iron-sulfur protein; THF, tetrahydrofolate; CoA, coenzyme A; EPR, electron paramagnetic resonance; XAS, X-ray absorption spectroscopy; EXAFS, X-ray absorption fine structure.

2. Low-temperature zero-field Mössbauer spectra of C_{red1} exhibit magnetic hyperfine interactions indicating a half-integer spin state, and high-temperature spectra exhibit the FCII doublet, with parameters of a ferrous ion. Four redox titrations of $CODH_{Ct}$ have been reported, all qualitatively similar (18,20,21,30). Although EPR-monitored titrations of $CODH_{Rr}$ have not been reported, its redox behavior appears to be similar (14). As potentials are lowered from ~ 0 mV, the C_{red1} EPR signal appears first, followed by B_{red} and then C_{red2} as C_{red1} declines (depending somewhat on the presence or absence of CO_2). Similar properties were also observed in pre-steady-state kinetic studies (21,38,39). In contrast, the Ludden model seems to imply that in such titrations, C_{red2B} should appear first, followed by C_{red1}, C_{unc} and finally C_{red2A}.

Metalloenzymes seem to "come of age" when their structures are known at atomic resolution, spectroscopic and catalytic properties are basically understood, and genetic expression systems are available. Such foundations allow detailed mechanistic and spectroscopic properties to be probed and correlated to structure. The objective of this article is to summarize what is known about the title group of enzymes, and show that, to a large degree, they have come of age. I apologize to those involved in aspects that I do not cover, or do so inadequately. Previous reviews should be consulted for other perspectives and emphases (1-5).

Ni-containing carbon monoxide dehydrogenases are phylogenetically related, but they vary in terms of metabolic role, subunit composition, and catalytic activity. Monofunctional enzymes that exclusively catalyze the reversible oxidation of CO to CO_2, reaction [1], are called *Carbon Monoxide Dehydrogenases* (CODH's)[1], and are specified by a subscript indicating the host organism. Bifunctional enzymes that additionally catalyze the synthesis of acetyl-CoA, reaction [2], are called acetyl-CoA synthases/carbon monoxide dehydrogenases (ACS/CODH's).

$$CO + H_2O \rightleftarrows CO_2 + 2e^- + 2H^+ \qquad [1]$$

$$CH_3\text{-}Co^{3+}FeSP + CO + CoASH \rightleftarrows CH_3C(O)SCoA + Co^{1+}FeSP + H^+ \qquad [2]$$

$$H^+ + Co^{1+}FeSP + CH_3\text{-}THF = CH_3\text{-}Co^{3+}FeSP + THF \qquad [3]$$

$$CH_3C(O)SCoA + H_4SPT + H_2O \rightleftarrows CH_3\text{-}H_4SPT + CO_2 + 2e^- + 2H^+ + CoASH \qquad [4]$$

CoFeSP in reaction [2] is the corrinoid-iron-sulfur protein, a heterodimer containing a cobalamin in one subunit and an Fe_4S_4 cluster in the other (1). Reduced Co^{1+} cobalamin accepts a methyl group from CH_3-THF in reaction [3], catalyzed by methyltransferase (6). Another group of bifunctional ACS/CODH's catalyze the decarbonylation of acetyl-CoA, reaction [4]. H_4SPT is tetrahydrosarcinapterin, an archaeal analog of THF.

These enzymes are housed in evolutionarily primitive organisms that can grow exclusively on simple inorganic compounds (7). Wächtershäuser has implicated ACS/CODH-like reactions as participating in the origin of life (8). Organisms that were present prior to the appearance of O_2 may have used these enzymes as "tools" for extracting energy from environments that increasingly contained energy-rich organic molecules (7). Organisms housing these enzymes play critical roles in the global carbon cycle (9), antibiotic-associated colitis and nosocomial infections (10), and the degradation of environmental pollutants (11).

The Ni-CODH family of enzymes can be divided into four classes (7). Class I enzymes are ACS/CODH's found in obligate autotrophic methanogens such as *Methanobacterium thermoautotrophicum*, where they synthesize acetyl-CoA from CO_2/H_2. Class II enzymes are ACS/CODH's involved in acetoclastic methanogenesis. Both Class I and II enzymes are composed of 5 different types of subunits ($\alpha\beta\gamma\delta\varepsilon$) as illustrated in Figure 1, Panel A. Class III enzymes are ACS/CODH's found in homoacetogens, and consist of two autonomous proteins, including an $\alpha_2\beta_2$ tetramer (ACS/CODH) and a $\gamma\delta$ heterodimer (CoFeSP). Class III α, β, γ, and δ subunits are homologous to the β, α, γ, and δ subunits of the Class I/II enzymes, respectively. The ε subunit of the Class I/II enzymes has no Class III homolog. Class IV enzymes are monofunctional α_2 homodimers where α is homologous to the α subunit of Class I/II enzymes and to the β subunit of Class III enzymes. Found in anaerobic CO-utilizing bacteria such as *Rhodospirillum rubrum* and *Carboxydothermus hydrogenoformans*, these monofunctional enzymes catalyze CO/CO_2 redox but not the synthesis or degradation of acetyl-CoA.

X-Ray Structure of the CODH from C. hydrogenoformans at 1.63 Å Resolution (12) and R. rubrum at 2.8 Å Resolution (13). The structures of these two proteins are basically equivalent.

Both are ~130 kDa homodimers with a transverse two-fold rotation axis (Figure 1, Panel B). Dimers contain 5 metal-sulfur clusters of 3 types, called B, C, and D. The Fe_4S_4 D-cluster bridges the subunits and is located near the surface of the protein along the rotation axis. Each subunit contains another Fe_4S_4 cluster, called the B-cluster, located ~ 10 Å away from D. Extending ~ 11 Å further along each D—B cluster axis is the C-cluster *of the other subunit*. Viewed from one orientation, the C-B'-D-B-C' cluster arrangement has an inverted V shape with the D-cluster at the apex and a C-cluster at the base of each leg.

The only significant difference between the two structures is that of the C-cluster (Figure 2, middle structures). The $CODH_{Ch}$ structure was solved to significantly higher resolution than $CODH_{Rr}$ and it seems reasonable to assume that differences arise from uncertainties of fitting the lower resolution data. However, structural differences could also arise from differences in conditions used to crystallize the proteins, or from the protein structures themselves.

The Dobbek C-cluster (Figure 2, top structure) consists of 1 Ni, 4 Fe, and 5 sulfide ions. It is coordinated by 5 Cys residues (1 to each metal ion) and 1 His residue to one of the irons (almost certainly *Ferrous Component II* or FCII, see below (14)). The cluster can be divided into a [Ni-S-Fe] subsite (involving FCII) and an $[Fe_3S_4]$ subsite. Three sulfides of the $[Fe_3S_4]$ subsite constitute the *proximal face* and coordinate the metals of the [Ni-S-Fe] subsite. The *distal face*, composed of 3 Fe's and one μ^3 sulfide, points toward the B-cluster. The 3 proximal-face sulfides are also μ^3 (when linked to the [Ni-S-Fe] subsite) while the sulfide in the [Ni-S-Fe] subsite is μ^2. Each iron is 4 coordinate and tetrahedral. Each Fe of the $[Fe_3S_4]$ subsite has 4 S donors while the Fe of the [Ni-S-Fe] subsite has 3 S and 1 N donor. The Ni is 4-coordinate with 4 S donors arranged in a square plane. The Ni is displaced 0.3 Å above this plane. The Drennan C-cluster (Figure 2, multicolored middle) is essentially a $NiFe_3S_4$ cubane bridged to FCII.

The C-cluster is buried 18 Å below the surface of the protein. Small molecules probably come and go through a tunnel that extends from the ends of the protein dimer to the Ni of each C-cluster. From the C-cluster, the tunnel continues towards the B-cluster at which point it diverges toward the protein surface, bypassing the D-cluster.

Conserved Amino Acid Residues. Eighteen sequences of Class I/II/IV α subunits and Class III β subunits have been aligned (7), with selected regions shown in Table 1. Eight are Class I/II, including those from archaea *M. thermoautotrophicum*, *Methanococcus jannaschii* (sequence 1), *Archaeoglobus fulgidus* (sequences 1 and 2), *Methanosarcina frisia* (sequences 1 and 2), *Methanosarcina thermophila* and *Methanosaeta soehngenii*. Ten sequences are Class III/IV-like, from bacteria *R. rubrum*, *Clostridium thermoaceticum (also called Moorella thermoacetica)*, *C. hydrogenoformans*, *C. difficile* (sequences 1 and 2), *C. acetobutylicum* (sequences 1 and 2), and from archaea *A. fulgidus* (sequence 3), *M. jannaschii* (sequence 2) and *Methanopyrus kandleri*. Since the physiological function of the archaeon-housed "bacterial" enzymes is unknown, they are called "Class III/IV-like".

Cys ligands to the B-cluster are conserved throughout all sequences, but those to the D-cluster are not. Five D-ligating patterns can be discerned. Conserved residues are numbered differently for each protein and to avoid confusion we use the universal numbering scheme (7) in Tables 1 and 2 (supporting information). The arrangement characteristic of $CODH_{Ch}$ and $CODH_{Rr}$, in which Cys070 and Cys078 are D-cluster ligands, is also present in sequences from *C. thermoaceticum*, *C. difficile*, and *C. acetobutylicum* (sequence 2). The second pattern, in which Cys075 probably substitutes for Cys070, is found in all Class I/II sequences except for those from *M. soehngenii* and *A. fulgidus* (sequence 2). The pattern found in these two species

lacks any Cys residues that could bind a D-cluster. The fourth configuration, evident in *C. acetobutylicum* sequence 1 and in *A. fulgidus* sequence 3, may coordinate the D-cluster using Cys070 and Cys073. The fifth configuration, evident in the Class III/IV-like sequences from *M. kandleri* and *M. jannaschii* (sequence 2) has only one appropriate ligand for D-cluster coordination (Cys070). Thus, *D-cluster coordination appears highly variable, raising the possibility that this cluster is missing or altered in some CODH enzymes.*

C-cluster ligands are completely conserved except for those from *C. acetobutylicum* and *A. fulgidus* (sequence 2) which have Glu rather than Cys at position 335; in all other sequences Cys335 is a ligand to FCII. Except for these differences, *all CODH enzymes appear to contain C-clusters of uniform structure*. The majority of sequences exhibit a conserved His pattern involving positions 124, 127, 130, and 134 (or thereabout). His124 neighbors the [Ni-S-Fe] subsite of the C-cluster, while the other His residues are part of the tunnel (13), and could serve as a proton transfer relay. In some Class III/IV-like sequences, this pattern has changed (Table 1). Class I/II enzymes contains two additional regions, absent in Class III/IV-like sequences, that almost certainly support Fe_4S_4 clusters dubbed E- and F-clusters. These putative clusters might reroute electron transfer along different paths (7). Lys725 is conserved in all but 4 Class III/IV-like sequences, and has been proposed to stabilize M-COO^- by H-bonding (13). Other interesting residues are highlighted in Table 1.

In summary, CODH sequences can be divided into Class I/II and Class III/IV-like groups, and these can be further divided into 2 and 4 subdivisions, respectively. Some organisms contain multiple CODH-encoding genes, but in all cases they arise from different subdivisions. This suggests that *enzymes from different subdivisions play distinct metabolic roles*; i.e. the presence of two CODH's in an organism does not reflect simple redundancy.

Redox and Spectroscopic Properties of B- and D-Clusters. Most spectroscopic properties of the B- and C-clusters have been determined using ACS/$CODH_{Ct}$ and $CODH_{Rr}$, though qualitatively similar features of other homologs, including $CODH_{Ch}$ (15), suggest that these properties are universal. Prior to the crystal structure results, these enzymes had been known to contain B- and C-clusters but not the D-cluster. Crystal structure results confirmed that the C-cluster consisted of a Ni ion associated with an Fe-S cluster that contained 4 Fe's, with one of these Fe's (FCII) unique and coordinated with His (14,16). However, in contrast to the crystal structure, the spectroscopic model had the Ni ion bridged to an Fe_4S_4 cluster (14,16,17). How can the spectral properties of the enzyme now be reconciled with the structure?

Let's start with the EPR and Mössbauer studies contributed by the Münck, Ragsdale, Ludden and Lindahl groups (14,18,19). Under oxidizing conditions (E ~ +50 mV vs. NHE), the B- and C-clusters are in their diamagnetic oxidized states, B_{ox} and C_{ox}. As potentials are lowered to ~ -300 mV, these clusters are reduced to the B_{red} and C_{red1} states (20,21). B_{red} exhibit an EPR signal (g_{av} = 1.94) typical of $[Fe_4S_4]^{1+}$ clusters with S = ½ system spin states (18,20). Mössbauer components associated with such clusters corresponds to ~ 1.5 Fe_4S_4 clusters/monomer. The extra 0.5 clusters/monomer were previously unexplained, but may reflect the D-cluster. However, further studies are required to verify this.

The Precursor C-cluster. When grown on Ni-depleted nutrients under a CO atmosphere, the enzyme from *R. rubrum* ($CODH_{Rr}$*) is catalytically inactive and devoid of Ni (22). Full activity develops after reducing $CODH_{Rr}$* and incubating it with $NiCl_2$. $CODH_{Rr}$* must therefore contain a Ni-deficient form of the C-cluster (called C*) that can be converted to the native C-cluster.

Mössbauer studies show that C* is either an $[Fe_4S_4]^{2+/1+}$ cluster, or a novel structure that has EPR, Mössbauer and UV-vis features typical of such clusters. In the former case, activation would appear to involve a major structural rearrangement as Ni is inserted and a sulfide ion is sequestered from the environment.

Roberts and Ludden have studied the *coo* operon responsible for $CODH_{Rr}$ extensively, and have identified genes *cooCTJ* responsible for inserting the Ni into C* (23). The CooC homodimer binds and hydrolyzes ATP/GTP and inserts the Ni (24). CooJ contains a His-rich C-terminus that binds up to 4 Ni ions (25). CooT may be involved in metal ion discrimination (23). It is tempting to conclude that these proteins cause the major structural rearrangement suggested above, but recall that reduced $CODH_{Rr}$* can be activated *in-vitro* by simply adding $NiCl_2$.

Redox and Spectroscopic Properties of the C-cluster. At potentials below -200 mV, diamagnetic C_{ox} is reduced by 1 electron to the S = ½ C_{red1} state exhibiting an EPR signal with $g_{av} = 1.82$ (18,26). Mossbauer spectra reveal that C_{red1} contains 4 irons, two of which are called FCII and FCIII (2 irons could not be individually characterized). FCIII is a high-spin Fe^{2+} that, along with the uncharacterized irons, probably constitutes the $[Fe_3S_4]$ subsite. FCII is a high-spin 5- or 6-coordinate Fe^{2+}, and is almost certainly the Fe of the [Ni-S-Fe] subsite. ENDOR studies in the Hoffman lab indicate that a Histidine residue ligates FCII (16). CN^- is a potent tight-binding inhibitor of CO/CO_2 redox catalysis that binds to FCII in the C_{red1} state and displaces a strongly-coupled OH- group (14,16,27).

Since the late 80's, Ni was assumed to be associated with the C-cluster, but evidence for this was inconclusive. Adding Ni to $CODH_{Rr}$* perturbed the electronic spin state of C_{red}* and converted one of the irons of this precursor cluster into FCII (14). Hyperfine interactions

between the spin of C_{red1} and ^{61}Ni were reported (28), but could not be confirmed (14). L-edge XAS by Cramer and coworkers indicated a low-spin diamagnetic Ni^{2+} ion (29), a result supported by the square-planar geometry of the Dobbek structure. This diamagnetic Ni would not be part of the spin-coupling mechanism, explaining the insignificant ^{61}Ni hyperfine. This result, along with the absence of FCII in C_{ox} Mössbauer spectra, suggests that reducing C_{ox} to C_{red1} corresponds to reaction [5].

$$[Ni^{2+}\text{-S-}Fe^{3+}]\ (C_{ox}) + 1e^- = [Ni^{2+}\text{-S-}Fe^{2+}]\ (C_{red1}) \qquad [5].$$

To be compatible with the observed S = 0 and S = ½ spin states for C_{ox} and C_{red1}, respectively, the $[Fe_3S_4]$ subsite should have a 1- core oxidation state (i.e. $[Fe_3S_4]^{1-}$) for both C_{ox} and C_{red1}.

The coordination environment of the Ni in $CODH_{Rr}$ was investigated by K-edge XAS spectroscopy (17). A Ni-Fe interaction at 2.8 Å was observed for a well-characterized $[NiFe_3S_4]$ cubane model compound but not for the enzyme. The Ni in $CODH_{Rr}$ was reasonably concluded not to be incorporated into a cubane, but possibly bridged to an Fe-S cluster and coordinated by 2-3 N/O and 2 S ligands. Near edge studies suggested either tetrahedral or distorted geometry but not square planar. These results and conclusions are not easily reconciled with the crystal structures. The Dobbek C-cluster seems less rigid than a cubane and thus less likely to exhibit strong Ni-Fe interactions, but the observed all-sulfur square planar environment is difficult to reconcile with the Ni site proposed by the XAS study.

The C-cluster exhibits two additional redox states called C_{red2} and C_{int} (18,20,30,31). C_{red2} is S = ½ and exhibits an EPR signal similar to C_{red1} but with $g_{av} = 1.86$ (for ACS/$CODH_{Ct}$). The C_{red1}-to-C_{red2} conversion is redox-dependent and occurs (under an Ar atmosphere) in accordance with $E^{0'} = -540$ mV. Numerous low-potential reductants including CO and dithionite can effect this reduction. Spectroscopic characteristics of C_{red2} have been difficult to study because B- (and

probably D-) clusters are paramagnetic under conditions where C_{red2} is present (14). It is clear, however, that FCII is present in C_{red2} spectra, and that the strongly coupled OH^- evident in ENDOR studies of C_{red1} is absent (14,16).

Heterogeneity. Spin intensities of all well-characterized EPR signals in ACS/$CODH_{Ct}$, including those from B_{red}, C_{red1} and C_{red2} (and A_{red}-CO, see below) quantify to approximately 0.7, 0.3, 0.3 and 0.3 spin/$\alpha\beta$, respectively (18-20). These intensities are below unity because CODH samples are heterogeneous in terms of redox and spin states (20). My impression is that the problem occurs independently of laboratory and organism, though this is uncertain. Ludden and coworkers report that heterogeneity can be "cured" by preincubation with CO (32). Meyer's group reports ~ 1.1 spin/monomer for C-cluster signals in $CODH_{Ch}$ (15). Heterogeneity does not appear to arise from the process in which metal centers are built or installed into the protein. We recently cloned the genes encoding ACS/$CODH_{Ct}$, and expressed them in *Escherichia coli* (33). *E. coli* does not naturally contain enzymes in the CODH family, and thus presumably lacks the specific accessory proteins used by *C. thermoaceticum* in metal-center assembly/insertion. However, the resulting recombinant protein was catalytically active and exhibited EPR signals with the same low spin intensities as native enzyme. This suggests that heterogeneity arises from factors *inherent* to the enzyme. Might the presence of a single D-cluster per dimer be involved?

Mechanism of CO/CO_2 Redox Catalysis. The most popular mechanism of CO oxidation (12,13,14,16,34) has CO binding to the Ni of the C-cluster and H_2O binding to FCII (Figure 3, upper mechanism). This lowers the pK_a of the H_2O, yielding a nucleophilic OH^- that attacks the Ni-bound CO. Ni binding to CO increases the electrophilicity of the carbonyl carbon and may

induce dissociation of the OH^- (16). A base accepts a proton from the resulting Ni-bound carboxylic acid group, encouraging CO_2 to dissociate as two electrons are delivered to the enzyme. Electrons exit the enzyme one-at-a-time through the {B-cluster:D-cluster} "wire" (12,13) as protons exit through the histidine relay pathway.

Many details of this mechanism require further testing before it can be considered established. Among the most contentious are the site to which 2 electrons are delivered as CO_2 dissociates, as well as the redox and spin state of this site. One possibility is that C_{red2} is 2 electrons more reduced than C_{red1}, and that C_{red1} accepts the electrons (27,35), reaction [6].

$$[C_{red1}]^{n+} + CO + H_2O = [C_{red2}]^{(n-2)+} + CO_2 + 2H^+ \qquad [6]$$

Both states are S = ½ and thus may differ by 2 electrons, as required for catalyzing an n = 2 process. Moreover, $E^{0'}$ for the C_{red1}-to-C_{red2} transition (-0.51 V) is near that for the CO_2/CO couple (-0.512 V). If electrons exit the enzyme one at a time, this proposal implies that the C-cluster should be stable in a redox state $1e^-$ more reduced than C_{red1} and $1e^-$ more oxidized than C_{red2}. Evidence for such a state, called C_{int}, has been obtained (31). One problem with this possibility is the lack of an obvious site on the C-cluster to deposit those 2 electrons. The electronic state of C_{red2} is very similar to that of C_{red1}. A 2-electron reduction of C_{red1}, forming a state involving Ni^{1+} and an all-Ferrous $[Fe_3S_4]^{2-}$ subsite, would yield an electronic state substantially different than C_{red1}. An electronic state involving Ni^0 and $[Fe_3S_4]^{1-}$ would be similar to that of C_{red1} (as both d^{10} Ni^0 and low-spin d^8 Ni^{2+} would be diamagnetic) but there is no precedence for sulfide ions and thiolate groups supporting Ni^0. Could an electronically delocalized tri-thiolato ligand like the $[Fe_3S_4]^{1-}$ subsite stabilize Ni^0?

Ludden and coworkers have suggested a rather speculative mechanism that assumes spin-coupling in nearly all C-cluster states (32,36). The model was proposed before the crystal

structure was reported and it assumed some unrealized structural features (namely, that the C-cluster consisted of an $[Fe_4S_4]^{1+}$ cluster spin-coupled to an Ni-Fe binuclear center). In a "post-structure" publication, they retain the fundamentals of their model by viewing the unrealized Ni-Fe center as the [Ni-Fe] subsite and the unrealized $[Fe_4S_4]^{1+}$ cluster as the $[FeS_c]$ subsite (37). According to their model, C_{red2B} is an S = ½ state with an $[Fe^{2+}\ Ni^{2+}]$ subsite, C_{red1} is an S = 1 state that is 1 electron more reduced than C_{red2B} and has an $[Fe^{3+}\ Ni^{2+}\text{-}H^-]$ subsite, C_{unc} is an S = ½ state that is 1 electron more reduced than C_{red1} and has an $[Fe^{2+}\ Ni^{2+}\text{-}H^-]$ subsite, and C_{red2A} is isoelectronic with C_{unc} but has the $[FeS_c]$ subsite coupled to B_{red}. CO_2 reacts with C_{unc}, forming CO and C_{red2B} as products. Thus, C_{red2B}, C_{red1} and C_{unc} ($\equiv C_{red2A}$) of the Ludden model are equivalent in terms of redox state to C_{red1}, C_{int}, and C_{red2} states, respectively, in the "standard" mechanism. Characterizing C_{red1} as an even-spin state with Fe^{3+} in the [Ni-Fe] subsite is contrary to Mössbauer spectra of this state, and the order in which C-cluster EPR signals are proposed to develop and decay, according to the Ludden model, seem contrary to what is observed.[2]

Site-directed mutagenesis has been used to correlate C-cluster structure and function. Spangler et al. prepared a mutant $CODH_{Rr}$ in which Val replaces His299, an FCII ligand (26). H299V is 1000-times less active than native $CODH_{Rr}$, it contains sub-stoichiometric amounts of Ni, and does not exhibit the C_{red1}/C_{red2} EPR signals. These results demonstrate the importance of this ligand in catalysis and redox, and suggest a link between FCII and the ability of the cluster to coordinate Ni. A mutant was also prepared in which Ala replaced Cys675, a ligand to the Ni (36). The Ni content of C675A was similar to that of native $CODH_{Rr}$, but the mutant was inactive, and its Fe-S clusters were not reduced when C675A was exposed to CO. Also, EPR signals from the C_{red1}/C_{red2} states were replaced by a new signal with $g_{av} = 2.16$. Thus, C675

appear to be required for catalysis and redox, but not binding the Ni to the cluster. This is counterintuitive, given that Cys675 coordinates the Ni.

CO_2 effects. CO_2 alters many properties of the metal centers (30). Incubating ACS/$CODH_{Ct}$ in CO_2 increases $E^{0,}$ for the C_{red1}/C_{red2} conversion, $E^{0,}$ for the B_{ox}/B_{red} transition, and $E^{0,}$ for the A_{ox}/A_{red} transition. CO_2 perturbs the C_{red1} and B_{red} EPR signals, and it may convert $CODH_{Ct}$ into a form in which clusters are reduced by a cooperative process. In the presence of a low-potential reductant like dithionite, CO_2 increases the rates at which the C_{red1} converts to C_{red2} and that at which CN^- dissociates from FCII. It "cures" batches of defective enzyme that had been unable to reduce their C-clusters from the C_{red1} to C_{red2} states (35). CO_2 increases the strength of CO binding to the A-cluster (introduced below) by ~ 10-fold, and inhibits the CO/acetyl-CoA exchange activity of ACS/$CODH_{Ct}$. The binding of CO_2 appears to cause a significant conformational change that reconfigures the metal centers in the enzyme such that redox potentials are matched and reductions occur rapidly and synchronously. Pre-steady state kinetic evidence indicates that ACS/$CODH_{Ct}$ is activated for acetyl-CoA synthesis by CO_2 binding and a 2-4 electron reduction (40).

The Ludden group reported that $CODH_{Rr}$ is activated for CO/CO_2 redox catalysis by CO binding and a 1-electron reduction of a site having E^0 ~ -340 mV (37,41,42). In conflict with the standard model, they conclude that C_{red1} is not used in catalysis, as this state develops with E^0 = -110 mV in $CODH_{Rr}$ and is present at potentials at which the enzyme could not reduce CO_2. They suggest that C_{unc} binds and reduces CO_2. An important test of this would be to determine E^0 for the C_{red1}-to-C_{red2} conversion in $CODH_{Rr}$.

Redox and Spectroscopic Properties of the A-cluster. Enzymes that catalyze the synthesis or decarbonylation of acetyl-CoA contain another type of metal center called the A-cluster, which serves as the active site for these reactions. It is located in the α subunit of Class III-like enzymes and the β subunit of Class I/II enzymes (43-45). The A-cluster is stable in either of 2 oxidation states, including an S = 0 state called A_{ox} and an S = ½ state called A_{red}-CO. Converting A_{ox} to A_{red}-CO involves $1e^-$ reduction and CO binding. A_{red}-CO exhibits the NiFeC EPR signal, so named because incorporating ^{61}Ni (I = 3/2), ^{57}Fe (I = ½) and ^{13}CO (I=1/2) in this cluster hyperfine-broadens the signal. The elegant studies by Ragsdale, Wood, and Ljungdahl that demonstrated this provided the first evidence for a NiFe center in biology (1,46).

The basic structure of this cluster was determined using EPR, ENDOR, Mössbauer, model compound synthesis, and XAS spectroscopies (1,18,19,46,47,48), with the strongest evidence being that obtained once methods were developed to isolate α subunits from $ACS/CODH_{Ct}$ (43,44). This procedure allowed the spectroscopic properties of the A-cluster to be examined without interference from clusters in the β subunit. Isolated α subunits contain 4 Fe/α and exhibit EPR and UV-vis properties typical of $[Fe_4S_4]^{2+/1+}$ clusters. Treatment with aqueous Ni^{2+} yields a state that mimics the EPR, Mössbauer, CO binding and redox properties of A_{red}-CO, suggesting that the A-cluster consists of a Ni ion spin-coupled to an Fe_4S_4 cluster. Mössbauer and UV-vis spectroscopies were used to determine that the Ni ion is reduced from the 2+ to 1+ state in the reduction of A_{ox} to A_{red}-CO; thus, A_{ox} corresponds to $[Fe_4S_4]^{2+}$-X-Ni^{2+} and A_{red}-CO corresponds to $[Fe_4S_4]^{2+}$-X-Ni^{1+}-CO (43,44).

The intensity of the NiFeC signal corresponds to only ~ 0.3 spin/α, again significantly less than the expected value of unity. The Ni of the A-cluster is labile and can be removed by 1,10-phenanthroline (49). This eliminates acetyl-CoA synthase activity and the ability to

generate the A_{red}-CO state and the NiFeC signal. Reinsertion of Ni reactivates the enzyme and restores its ability to generate this state and signal. The amount of Ni removed and replaced (~ 0.3 Ni/$\alpha\beta$) suggests that only ~ 30% of A-clusters have labile Ni ions, are catalytically active and can exhibit the NiFeC EPR signal (43,49). The remainder have nonlabile Ni ions, do not exhibit the NiFeC signal, and are inactive.

Methylation of ACS_{Ct}. A methylated form of ACS_{Ct} can be prepared by treating *reduced* enzyme with CH_3-Co^{3+}FeSP (1,50). The A-cluster is almost certainly the site to which the methyl group binds, but the species that must be reduced before methyl transfer occurs remains uncertain. This species was initially assumed to be the A-cluster itself, but Barondeau and Lindahl found that reductants unable to reduce A_{ox} *can* effect methylation (50). Other known redox sites on the enzyme were also eliminated, suggesting that ACS_{Ct} contains an unidentified n = 2 redox site which they called the *D-site* (not related to the D-cluster). They proposed that D was a redox-active disulfide, and designated activation and methyl group transfer from CH_3-Co^{3+}FeSP to be those shown in reactions [7] and [8].

$$[Ni^{2+}\ D_{ox}]^{n+} + 2e^- \quad = \quad [Ni^{2+}\ D_{red}]^{(n+2)+} \qquad [7]$$

$$CH_3\text{-}Co^{3+}FeSP + [Ni^{2+}\ D_{red}]^{(n+2)+} = Co^{1+}FeSP + [CH_3\text{-}Ni^{2+}\ D_{ox}]^{(n+1)+} \qquad [8].$$

The methyl group transfers as a CH_3^+ cation and most likely involves an S_N2 nucleophilic displacement (1,51), and is unusual because it involves metal ions as both methyl group donor and acceptor. D is a surrogate redox agent that allows the Ni to remain in the 2+ state upon methylation. The $\{Ni^{2+}D_{red}\}$ unit is comparable to Co^{1+} cobalamin in terms of nucleophilicity and can be viewed as the functional equivalent of "Ni^0".

Proposed Structure of the A-cluster. The proposed structure for the Ni-labile form of the A-cluster is shown (Figure 2, bottom) with methyl group and CO bound, and with a Cys bridging ligand. In the A_{ox} state, the Ni is 4-coordinate with S_2N_2 donors and two *cis* open coordination sites. This arrangement is suggested because in organometallic complexes, CO inserts into metal methyl bonds in which the methyl is bound on the same metal *cis* to the CO. It also rationalizes why 1,10-phenanthroline can remove Ni from this cluster. The non-bridging coordinated Cys sulfur forms a disulfide bond with another Cys, and this constitutes D_{ox}. Sequence alignment reveals that 6 Cys, 3 His, 1 Met, and numerous Asp/Glu residues are conserved (7). Three of these Cys residues probably coordinate the Fe_4S_4 portion of the A-cluster, 1 might bridge the cluster and Ni, and 2 might constitute the D-site. The Met and 2 His residues could also coordinate the Ni, while the remaining His could be used as a base for deprotonating CoA (52). The Ni of the A-cluster and the Co of the CoFeSP are probably at the surface of their respective proteins, as the methyl group probably transfers directly from one metal to the other.

Proposed Catalytic Mechanism of Acetyl-CoA Synthesis. We favor the following mechanism (50,44,52) (Figure 3, lower mechanism). The D-site is reduced by $2e^-$, CH_3-Co^{3+}FeSP binds ACS/$CODH_{Ct}$ and a methyl cation transfers to Ni^{2+} as D is oxidized. Then CO binds to the Ni^{2+} and inserts into the CH_3-Ni^{2+} bond, forming a $CH_3C(O)$-Ni^{2+} group. A base abstracts the thiol proton of CoA and the resulting thiolate attacks the carbonyl group of the acetyl-Ni^{2+} group. Finally, D_{ox} is re-reduced as acetyl-CoA eliminates. CO insertion and reductive elimination steps are common to organometallic chemistry, but are rare in biology. This mechanism has been embellished through the years but is derived from the seminal study of Wood and Ragsdale (53). Tucci and Holm's well-characterized reaction sequence using Ni model complexes (47)

was also critically important in developing this model. Whether substrates react in the order proposed has not been established. However, CoA probably reacts last, since the species with which it reacts (acetyl-Ni^{2+}) is formed from the reaction of the other two substrates. Other mechanisms employ the A_{red}-CO state as a catalytic intermediate (1), but there is evidence that this state inhibits catalysis (50,54). Further studies are required to resolve this.

Tunnel Connecting the C- and A-clusters, and A→C Coupling. Maynard and Lindahl discovered that as long as ACS_{Ct} is reduced, CO_2 can be used as a substrate in the synthesis of acetyl-CoA (54). In this case, CO is generated at the C-cluster by the reduction of CO_2 and it travels to the A-cluster where it is used in acetyl-CoA synthesis. Catalysis is unaffected when hemoglobin is included in assays as a CO "sponge", suggesting that the CO generated at the C-cluster migrates to the A-cluster through a proteinatious tunnel. Similar tunnels are found in other bifunctional enzymes in which the product of one reaction is the substrate of the other.

Effects of changing CO/CO_2 concentrations on steady-state acetyl-CoA rates show that CO activates ACS_{Ct} at low concentrations (~ 10 μM), is a substrate at intermediate concentrations (K_M ~ 300 μM), and is an inhibitor at high concentrations (K_I's ~ 50 to 900 μM) (55). Substrates CO and CO_2 compete for the C-cluster, while inhibitor CO molecules bind cooperatively to a form of the enzyme that differs from that to which substrate CO and CO_2 bind. Substrate CO may migrate to the A-cluster from the C-cluster via the tunnel while inhibitor CO may bind directly to the A-cluster (and form A_{red}-CO) without going through the tunnel.

This raises the issue of whether the two active sites are coordinated in terms of kinetics and mechanism. k_{cat} and K_M for CO_2 reduction are 37 min^{-1} and 7 mM, respectively, while during synthesis of acetyl-CoA (with CH_3-Co^{1+}FeSP and CoA included), the equivalent

parameters are 200 min^{-1} and 380 μM, respectively (40). Thus, the apparent second-order rate constant for CO_2 consumption increases ~100 fold when ACS/$CODH_{Ct}$ converts from reductase to synthase "mode"! Binding of the synthase substrates CoFeSP and CoA triggers this effect, and the conversion occurs with k_{app} ~ 80 min^{-1}. Triggering, communication of information, and alteration of kinetic parameters are collectively referred to as *A→C coupling*. By monitoring CO production (using hemoglobin as a CO detector), Maynard and Lindahl found that A→C coupling precludes the release of CO from the enzyme (40). Coupling *reroutes* CO that is produced at the C-cluster through the tunnel and to the A-cluster, *synchronizing* rates of the two activities. An ordered mechanism could synchronize events occurring at the two distant active sites. Thus, ACS/$CODH_{Ct}$ operating in synthase mode using CO_2 as a substrate may be viewed as having a single active site composed of a Cobalamin:A-cluster:Tunnel:C-cluster unit.

Class I/II subunit properties are now understood (56-58). The acetyl group of acetyl-CoA transfers to the Ni on the A-cluster of the β subunit. CO is eliminated and migrates to the α subunit where it is oxidized to CO_2. The γδ subunits transfer the methyl group to H_4SPT via an CH_3-Co^{3+} cobalamin intermediate. Grahame developed an assay catalyzed by the ACS/CODH of *M. barkeri* in which 3'-dephosphoCoA (CoA*) exchanges with CoA in acetyl-CoA (56).

$$\text{Acetyl-CoA} + \text{CoA*} = \text{Acetyl-CoA*} + \text{CoA} \qquad [9].$$

The enzyme is reductively activated (E^0 = -486 mV, pH 6.5) in a step that involving H^+ transfer (possibly corresponding to the reduction of the D-site). Reaction [9] occurred by a ping-pong mechanism, indicating the presence of an acetyl-enzyme intermediate. This high-energy intermediate has $\Delta G^{0'}$ of hydrolysis = –9.5 kcal/mol.

Future Directions. The complexity and functional unity of the metal center structures, tunnels, and catalytic mechanisms employed by the CODH family of enzymes is impressive. Compared to what was known 20 years ago, the advances made have been significant and we seem justified in proclaiming that these enzymes have "come of age". On the other hand, compared to what is known about the best-understood enzymes, we can only see a faint light at the end of a long tunnel. Atomic level structures of acetogenic and methanogenic systems are required to advance our structural understanding of these enzymes, while further kinetic, spectroscopic and redox studies are required to improve our understanding of their catalytic mechanisms. One fascinating aspect of these enzymes is their use of nickel. What special properties of Ni provide a selective advantage to organisms that use it? We have a partial answer – Ni (in conjunction with Fe and S) allows organometallic type reactions to occur in biological systems – but a more complete answer requires further studies. Another important issue is what to do with this knowledge once we have it. Could uncovered principles of catalysis help synthesize new catalysts with useful properties? Might it be possible to genetically alter these enzymes to degrade toxic compounds? Such applications will hopefully follow as that light at the end of the tunnel shines brighter.

Acknowledgement. I sincerely thank all of my students and post-docs that have researched these enzymes in my laboratory, for both their work and friendship.

Supporting Information Available. A table of selected residues in $CODH_{Ch}$ and $CODH_{Rr}$ cross-referenced to the universal identification numbers, and indication of possible function is included. This material is available free of charge via the Internet at http://pubs.acs.org.

References:

1. Ragsdale, S. W. and Kumar, M. (1996) *Chem. Rev*. *96*, 2515 - 2539.

2. Ferry, J. G. (1995) *Ann. Rev. Microbiol*. *49*, 305 - 333.

3. Wood, H.G. and Ljungdahl, L.G. (1991), in *Variation in Autotrophic Life* (Shively, J. M., Barton, L. L., Eds.) Academic Press, N.Y. pp. 201 – 250.

4. Fontecilla-Camps J.C. and Ragsdale S.W. (1999) *Adv. Inorg. Chem*. *47*, 283-333.

5. Ermler, U., Grabarse, W., Shima, S., Goubeaud, M. and Thauer, R. K. (1998) *Curr. Opin. Struct. Biol.* 8, 749-758.

6. Seravalli, J., Zhao, S.Y. and Ragsdale, S.W. (1999) *Biochemistry*, *38*, 5728-5735.

7. Lindahl, P.A. and Chang, B. (2001) *Origins Life Evolution Biosphere*, *31*, 403-434

8. Huber, C., Wächtershäuser, G. (1997), *Science*, *276*, 245 - 247.

9. Bartholomew, G.W. and Alexander, M. (1979) *Appl. Environ. Microbiol*., *37*, 932-937.

10. Taege, A. J. and Adal, K.A. (1999), C*leveland Clinic Journal of Medicine 66*, 503 – 507.

11. Huang, S., Lindahl, P.A., Wang, C., Bennett, G.N., Rudolf, F.B., and Hughes, J.B. (2000), *Applied and Environmental Microbiology*, 66, 1474-1478.

12. Dobbek H., Svetlitchnyi, V., Gremer, L., Huber, R., Meyer, O. (2001) *Science* 293, 1281-1285.

13. Drennan, C. L., Heo, J., Sintchak, M.D., Schreiter, E., Ludden, P.W. (2001) *Proc. Natl. Acad. Sci. USA*., *98*, 11973-11978.

14. Hu, Z., Spangler, N. J., Anderson, M. E., Xia, J. Q., Ludden, P. W., Lindahl, P.A., and Münck, E. (1996) *J. Am. Chem. Soc*., *118*, 830 - 845.

15. Svetlitchnyi V., Peschel C., Acker G., Meyer O. (2001) *J. Bacteriol*. 183, 5134-5144.

16. DeRose, V. J., Anderson, M. E., Lindahl, P. A. and Hoffman, B. M.(1998) *J. Am. Chem. Soc.*, *120*, 8767 - 8776.

17. Tan, G. O., Ensign, S. A., Ciurli, S., Scott, M. J., Hedman, B., Holm, R. H., Ludden, P. W., Korszun, Z. R., Stephens, P. J., and Hodgson, K. O. (1992) *Proc. Natl. Acad. Sci. U.S.A. 89*, 4427 - 4431.

18. Lindahl, P.A., Münck, E. and Ragsdale, S.W. (1990) *J. Biol. Chem. 265*, 3873 - 3879.

19. Lindahl, P.A., Ragsdale, S.W. and Münck, E.(1990) *J. Biol. Chem. 265*, 3880 - 3888.

20. Fraser, D. M. and Lindahl, P.A. (1999) *Biochemistry*, *38*, 15697-15705.

21. Saravalli, J., Kumar, M., Lu, W.-P., and Ragsdale, S.W. (1997) *Biochemistry*, 36, 11241-11251.

22. Ensign, S.A., Campbell, M.J., Ludden, P.W. (1990) *Biochemistry*, *29*, 2162-2168.

23. Kerby, R.L., Ludden, P.W., Roberts, G.P. (1997) J. Bacteriol. 179, 2259-2266.

24. Jeon, W. B., Cheng, J., and Ludden, P.W. (2001) *J. Biol. Chem*., *276*, 38602-38609.

25. Watt, R.K., and Ludden, P.W. (1998) *J. Biol. Chem*., *273*, 10019-10025.

26. Spangler, N.J., Meyers, M.R., Gierke K.L., Kerby, R.L., Roberts G.P., and Ludden P.W. (1998) *J. Biol. Chem*., *273*, 4059-4064.

27. Anderson, M.E. and Lindahl, P.A. (1994) *Biochemistry*, *33*, 8702 - 8711.

28. Stephens, P.J., McKenna, M.-C., Ensign, S.A., Bonam, D. and Ludden, P.W. (1989) *J. Biol. Chem.*, *264*, 16347-16350.

29. Ralston C.Y., Wang H.X., Ragsdale S.W., Kumar M., Spangler N.J., Ludden P.W., Gu W., Jones R.M., Patil D.S. and Cramer S.P. (2000) *J. Am. Chem. Soc.,* 122, 10553-10560.

30. Russell, W. K., and Lindahl, P.A. (1998) *Biochemistry*, *37*, 10016-10026.

31. Fraser, D.M. and Lindahl, P.A. (1999), *Biochemistry*, *38*, 15706-15711.

32. Heo, J., Staples, C.R., Telser, J., and Ludden P.W. (1999) *J. Am. Chem. Soc*., *121*, 11045-11057.

33. Loke, H.-K., Bennett, G., and Lindahl, P.A. (2000) *Proc. Natl. Acad. Sci. USA*, *97*, 12530-12535.

34. Seravalli, J., Kumar, M., Lu, W.P., and Ragsdale, S.W. (1995), *Biochemistry*, *34*, 7879-7888.

35. Anderson, M.E. and Lindahl, P.A. (1996) *Biochemistry, 35*, 8371-8380.

36. Staples, C. R., Heo, J., Spangler, N. J., Kerby, R. L., Roberts, G. P. and Ludden, P. W. (1999), *J. Am. Chem. Soc. 121*, 11034 - 11044.

37. Heo, J., Halbleib, C.M., and Ludden, P.W. (2001), *Proc. Natl. Acad. Sci. USA* 98, 7690-7693.

38. Kumar, M., Lu, W.-P., Liu, L., and Ragsdale, S. W. (1993) *J. Am. Chem. Soc. 115*, 11646-11647.

39. Seravalli, J. and Ragsdale, S.W. (2000) *Biochemistry*, *39*, 1274-1277.

40. Maynard, E. L. and Lindahl, P.A. (2001) *Biochemistry*, *40*, 13262-13267.

41. Heo, J., Staples, C.R., and Ludden, P.W. (2001) *Biochemistry*, *40*, 7604-7611.

42. Heo, J., Staples, C.R., Halbleib, C.M., and Ludden, P.W. (2000) *Biochemistry*, *39*, 7956-7963.

43. Xia, J., Hu, Z., Popescu, C., Lindahl, P.A., and Münck, E. (1997) *J. Am. Chem. Soc.*, *119*, 8301-8312.

44. Russell, W. K., Stålhandske, C. M. V., Xia, J., Scott, R. A., and Lindahl, P.A. (1998) *J. Am. Chem. Soc*., *120*, 7502 - 7510.

45. Grahame, D.A., and DeMoll, E. (1996) *J. Biol. Chem*. *271*, 8352-8358.

46. Ragsdale, S.W., Wood, H.G., and Antholine, W.E. (1985) *Proc. Natl. Acad. Sci. U.S.A.* *82*, 6811-6814.

47. Tucci, G.C., and Holm, R.H. (1995) *J. Am. Chem. Soc*., *117*, 6489-6496.

48. Fan, C.L., Gorst, C.M., Ragsdale, S.W., and Hoffman, B.M. (1991), *Biochemistry*, 30, 431-435.

49. Shin, W., Anderson, M.E., and Lindahl, P.A. (1993) *J. Am. Chem. Soc.*, *115*, 5522-5526.

50. Barondeau, D. P., and Lindahl, P. A. (1997), *J. Am. Chem. Soc., 119*, 3959-3970.

51. Kumar, M., Qiu, D., Spiro, T.G., and Ragsdale, S.W. (1995) *Science*, 270, 628-630.

52. Wilson B.E., and Lindahl, P.A. (1999) *J. Biol. Inorg. Chem.*, *4*, 742 - 748.

53. Ragsdale, S.W., and Wood, H.G. (1985) *J. Biol. Chem*. 260, 3970-3977.

54. Maynard, E.L., and Lindahl, P.A. (1999) *J. Am. Chem. Soc*., 121, 9221-9222.

55. Maynard, E.L., Sewell, C., and Lindahl, P.A. (2001) *J. Am. Chem. Soc.*, *123*, 4697-4703.

56. Bhaskar, B., DeMoll, E., and Grahame, D.A. (1998) *Biochemistry 37*, 14491-14499.

57. Grahame, D. A., and DeMoll, E. (1996) *J. Biol. Chem. 271*, 8352 - 8358.

58. Maupin-Furlow, J. A., and Ferry, J. G. (1996) *J. Bacteriol*., *178*, 340 – 346.

Table 1. Sequence alignment of the subunit containing B-, C-, and D-clusters. Lines separate sequences into 6 patterns.

ORGANISM	CLASS	RESIDUE NUMBER (UNIVERSAL)						
		070----------087	123----------137	228	251	297	333	
M.thermoautotrophicum	I	FYAPF**C**DM**CC**…L**C**TYGK**C**	A**H**AG**H**AR**H**LVD**H**LIE	SAC**H**	M**D**…D	IG**H**N	I**CC**	
M. jannaschii I	I	FYMPI**C**DL**CC**…L**C**TFGK**C**	**CH**AG**H**SR**H**LV**HH**LIE	SAA**H**	I**D**…D	IG**H**N	I**CC**	
A. fulgidus I	I or II	FYAPA**C**DM**CC**…L**C**TMGK**C**	A**H**TG**H**AR**H**ML…**H**DIE	DAV**H**	L**D**…S	IG**H**H	I**CC**	
M. frisia I	I or II	VVTPM**C**DQ**CC**…Y**C**TYGP**C**	**CH**AA**H**GR**H**LLD**H**LIE	ATV**H**	L**D**…H	IG**H**N	L**CC**	
M. frisia II	II or I	VVTPM**C**DQ**CC**…Y**C**TYGP**C**	**CH**AA**H**GR**H**LLD**H**LIE	ATV**H**	L**D**…H	IG**H**N	L**CC**	
M. thermophila	II	VITPM**C**DQ**CC**…Y**C**TYGP**C**	**CH**AA**H**GR**H**LLD**H**LIE	ATV**H**	L**D**…H	IG**H**N	L**CC**	
M. soehngenii	II	MYSPADDT…**C**TL**C**TYGP**C**	A**H**TA**H**GR**H**LY…**H**WCL	AAC**H**	I**D**…S	YG**H**N	V**CC**	
A. fulgidus II	II or I	FYAPMQDF…**C**NL**C**TMGP**C**	A**H**TA**H**AR**H**LVD**H**LIE	**H**ST**H**	A**D**…H	VG**H**N	L**CC**	
R. rubrum	IV	**C**GFGSAGL**CC**RI**C**LKGP**C**	A**H**SE**H**GR**H**IALAMQ**H**	SRT**H**	A**D**…L	NG**H**N	I**CC**	
C. thermoaceticum	III	**C**KIGYEGI**CC**RF**C**MAGP**C**	A**HC**E**H**GN**H**IA**H**ALVE	NQA**H**	A**D**…Y	**H**G**H**N	I**CC**	
C. hydrogenoformans	IV	**C**GFGETGL**CC**RH**C**LQGP**C**	G**H**SG**H**AK**H**LA**H**TLKK	**H**RTS	A**D**…L	**H**G**H**N	I**CC**	
C. difficile I	III or IV	**C**GFGLQGV**CC**RI**C**GMDP**C**	A**H**SD**H**ARDIA**H**TL…A	**H**ST**H**	A**D**GW	**H**G**H**E	M**CC**	
C. acetobutylicum I	III or IV	**C**KF**C**LEGLS**C**QL**C**SNGP**C**	TYS**HH**AYEAYRTLKA	ASCL	AT…I	NG**H**Q	SIE	
A. fulgidus III	III or IV	**C**PF**C**EKGLS**C**QL**C**SMGP**C**	AYTY**H**AIEAAKTLKA	SSAM	AT…C	NG**H**E	FIE	
C. acetobutylicum II	III or IV	**C**KFGKDGV**CC**KL**C**ANGP**C**	**C**YV**H**VVETTARNLKA	VKTS	STGL	TG**H**Q	**CTC**	
C. difficile II	III or IV	**C**GFGLQGV**CC**RL**C**SNGP**C**	**C**YL**H**VVENTAKNLKN	VKSS	STGL	TG**H**Q	**CTC**	
M. jannaschii II	III/IV?	**C**PYGLKGVY**C**IL**C**ANGP**C**	**C**YV**HC**AENAARALLS	TKTS	HAGF	TG**H**Q	AT**C**	
M. kandleri	III/IV?	**C**PYGKQGVW**C**NI**C**SNGP**C**	**C**YV**HC**LENAARALKS	VKTS	ITG…	TG**H**Q	AT**C**	

ORGANISM	CLASS	RESIDUE NUMBER (UNIVERSAL)					
		485----------495	526----------536	671----------680	724	731	741
M.thermoautotrophicum	I	**C**TD**C**GW**C**QRV**C**	**C**YT**C**GR**C**EQE**C**	NMGS**C**VSNA**H**	Q**K**A	TGV	VLGP**H**
M. jannaschii I	I	**C**TE**C**GW**C**NRN**C**	**C**YG**C**GR**C**EAI**C**	NCGS**C**LSNC**H**	Q**K**A	TGV	ILGP**H**
A. fulgidus I	I or II	**C**TQ**C**GN**C**TIA**C**	**C**IA**C**GR**C**EQV**C**	QIGS**C**VANA**H**	Q**K**A	TGF	VVGP**H**
M. frisia I	I or II	**C**AD**C**GA**C**YLA**C**	**C**IG**C**RR**C**EQV**C**	NIGS**C**VSNA**H**	Q**K**A	TGC	VLGA**H**
M. frisia II	II or I	**C**AD**C**GA**C**LIA**C**	**C**IG**C**RR**C**EQV**C**	NIGS**C**VSNA**H**	Q**K**A	TGC	VLGP**H**
M. thermophila	II	**C**AD**C**GS**C**YLV**C**	**C**IG**C**RR**C**EQV**C**	NIGS**C**VSNA**H**	Q**K**A	TGC	VLGP**H**
M. soehngenii	II	**C**TE**C**NQ**C**AFV**C**	**C**VG**C**QR**C**EQT**C**	NIGS**C**VANA**H**	Q**K**A	TGV	VVQPS
A. fulgidus II	II or I	**C**TQ**C**MN**C**VFT**C**	**C**LA**C**MK**C**EQA**C**	NTGS**C**VANS**H**	H**K**A	TGF	VVGP**H**
R. rubrum	IV	……	……	**H**MGS**C**VDNSR	E**K**A	S**W**A	**H**VGSV
C. thermoaceticum	III	……	……	**H**MGS**C**VDNSR	G**K**A	T**W**W	**H**VGTM
C. hydrogenoformans	IV	……	……	**H**MGS**C**VHNSR	E**K**A	T**W**A	**H**IGVF
C. difficile I	III or IV	……	……	**H**MGS**C**VDISR	E**K**A	CYV	YLGIM
C. acetobutylicum I	III or IV	……	……	SFGT**C**TDTGR	Q**K**A	IFA	**H**LSPT
A. fulgidus III	III or IV	……	……	SFGT**C**TDTGR	Q**K**A	VFA	**H**VSPV
C. acetobutylicum II	III or IV	……	……	NFGP**C**LAIGR	E**Q**A	AFG	**H**LAIS
C. difficile II	III or IV	T……	……	NFGP**C**LAIGR	E**Q**A	AFG	**H**LALP
M. jannaschii II	III/IV?	……	……	NFGA**C**LSIAR	E**Q**A	TYA	**H**VSPV
M. kandleri	III/IV?	……	……	**H**YGP**C**LAIGK	E**Q**A	SSA	**H**VSPV

Figure Legends

Figure 1. Panel A. Subunit relationships among the four classes of CODH's. The switch in α and β designations in Class I/II vs. Class III enzymes arises because of relative molecular mass differences. Class I/II α contain extra regions that house the putative E and F clusters, and are thus larger than the homologous subunits. Class I/II β lacks a 30 kDa N-terminus region present in Class III homologs. Other details are given in the text. Panel B. Structure of homodimeric $CODH_{Rr}$ (13). Protein residues that obscured the view of the metal-sulfur clusters are not shown. $CODH_{Ch}$ has a similar overall structure (12).

Figure 2. Structures of the Ni-Fe-S Clusters in CODH's. Top Structure: The Dobbek C-cluster (14). Color code: Ni, green; Fe, rust-colored; S, yellow; N, blue, C, purple. Middle Structures: The Drennen C-cluster (multicolored) (13) with the Dobbek C-cluster (light blue) superimposed. The similarities between the two structures are remarkable. The only significant difference is the sulfur ion(s) that bridge(s) the Ni and FCII and an extra unidentified ligand to the Ni. Color code is the same as above, with the unidentified ligand in pink. Bottom Structure: The *proposed* structure of the A-cluster, shown with methyl group and CO coordinated. The structure includes an Fe_4S_4 cubane bridged through a Cys sulfur to a Ni center. Other ligands to the Ni include two His nitrogens and a sulfur ion from the D-site cystine (shown here in the D_{ox} state). Color code as above, but also: O, red; H, white.

Figure 3. Proposed catalytic mechanisms for the oxidation of CO and reduction of CO_2, and for the synthesis of acetyl-CoA. See text for details.

Figure 1

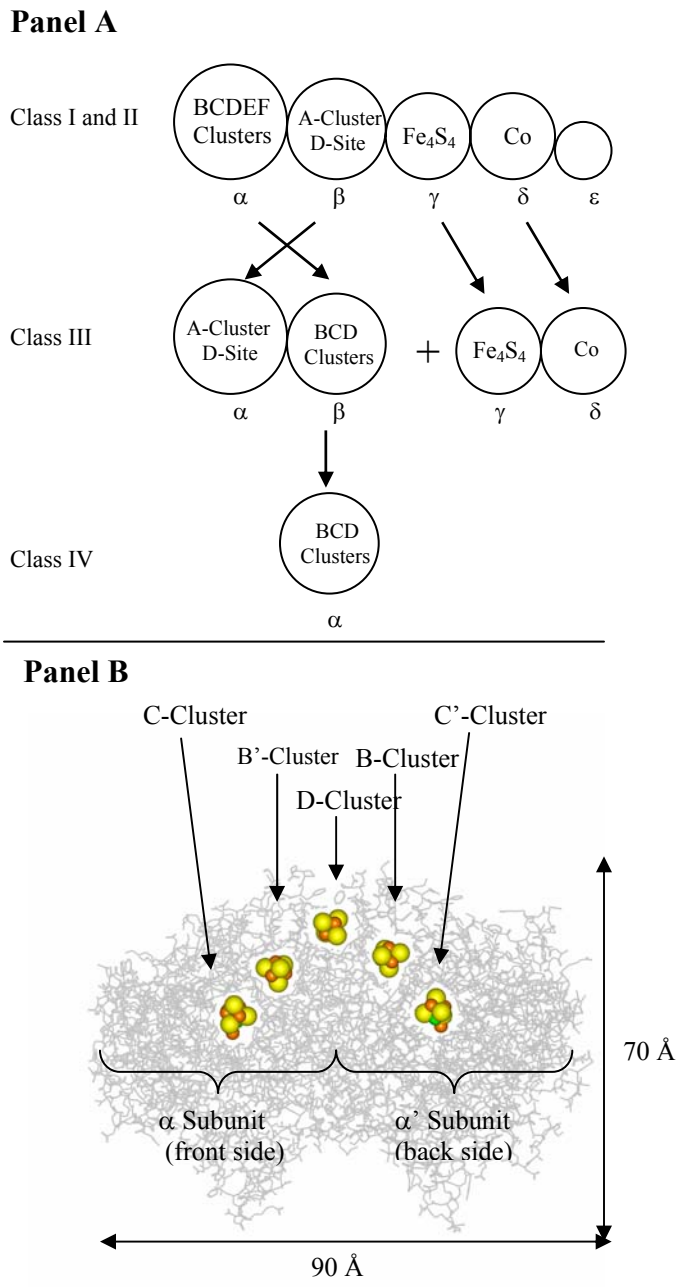
Panel A
Class I and II
BCDEF Clusters
A-Cluster D-Site
Fe4S4
Co
α
β
γ
δ
ε
Class III
A-Cluster D-Site
BCD Clusters
+
Fe4S4
Co
α
β
γ
δ
Class IV
BCD Clusters
α
Panel B
C-Cluster
C'-Cluster
B'-Cluster
B-Cluster
D-Cluster
70 Å
α Subunit (front side)
α' Subunit (back side)
90 Å

Figure 2

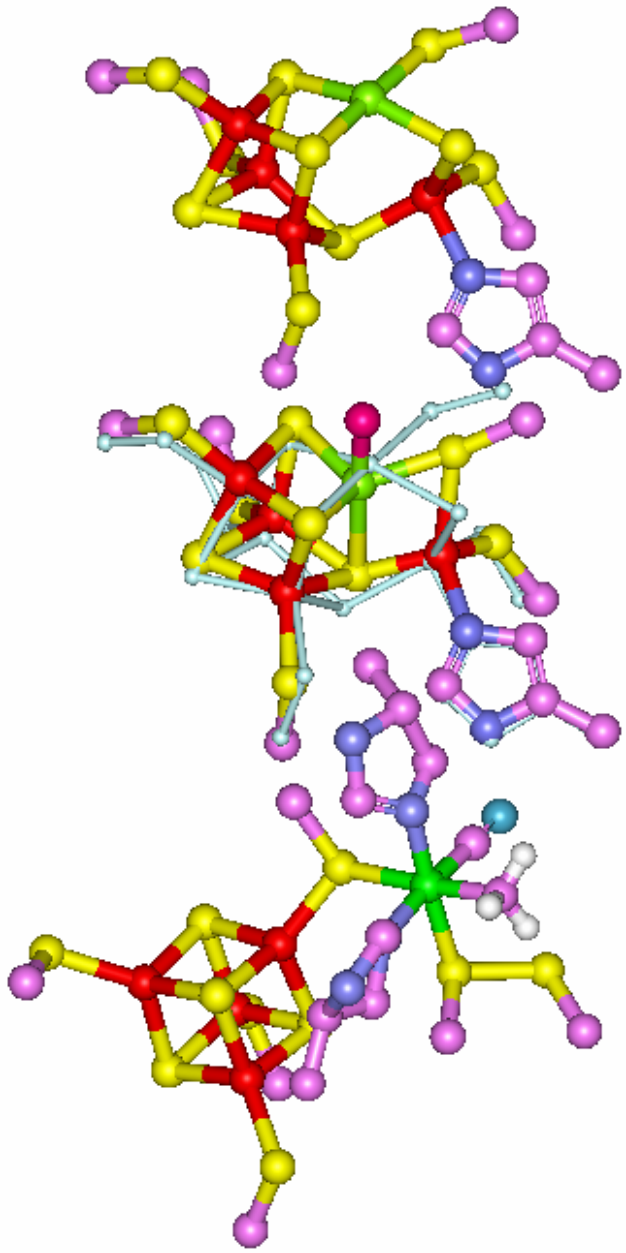

Figure 3

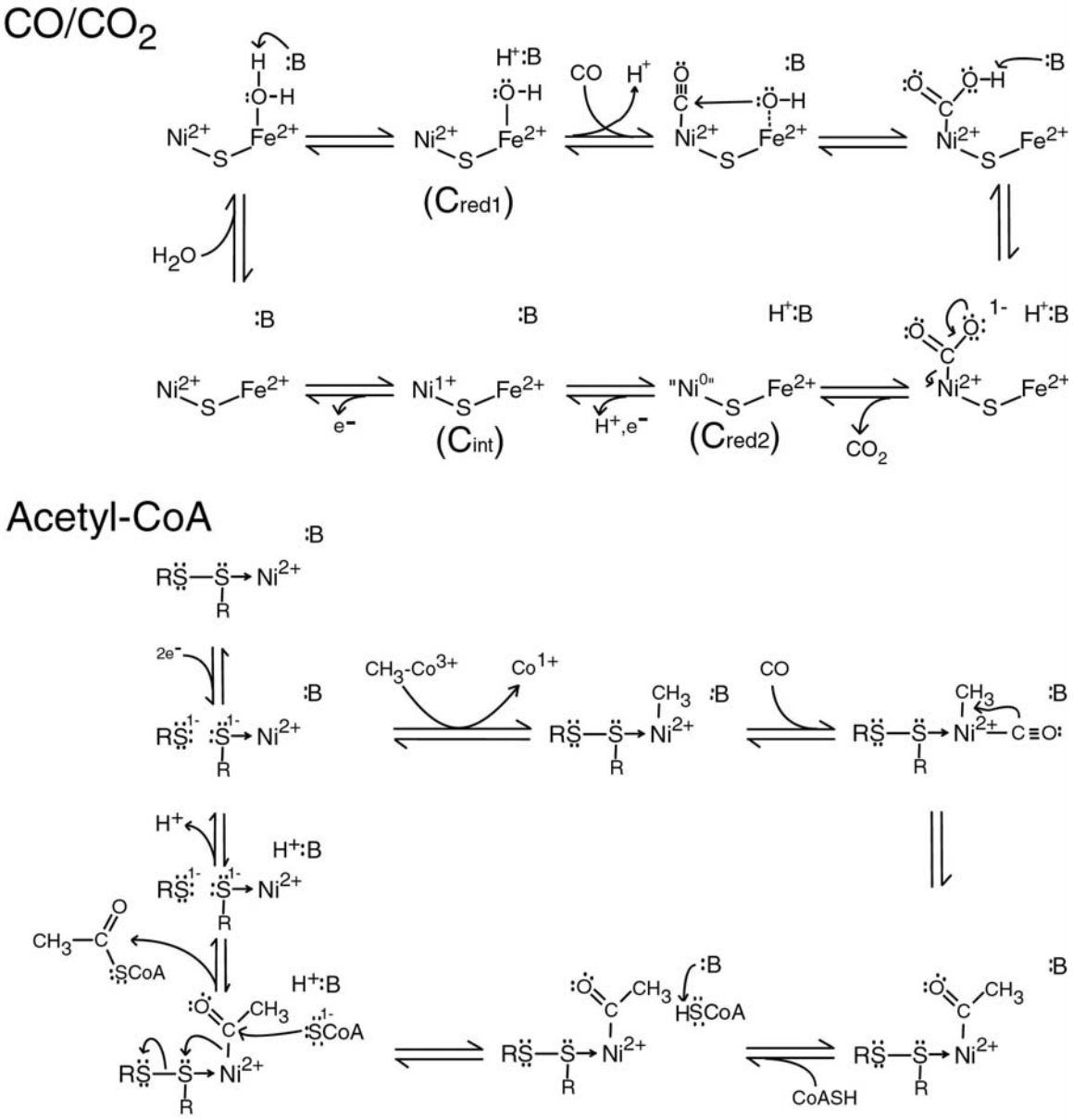

Supporting Information for World Wide Web Edition

Table 2: Selected Residues in $CODH_{Ch}$, $CODH_{Rr}$. Universal numbers (7) and a description of the residues are included.

Residue	$CODH_{Ch}$	$CODH_{Rr}$	Universal	Description
Cys	039	041	070	Ligand to D-cluster
Cys	047	049	078	Ligand to D-cluster
Cys	048	050	079	Ligand to B-cluster
Cys	051	052	082	Ligand to B-cluster
Cys	056	058	087	Ligand to B-cluster
Cys	070	072	101	Ligand to B-cluster
His	093	095	124	His pattern (H-bonded to Lys725?)
His	096	098	127	His pattern
His	099	101	130	His pattern
His	102	108	133/134	His pattern
His	195	202	231	Conserved in Class I/II some III/IV
Asp	219	223	252	(H-bonding Network)
His	261	265	299	Ligand to FCII of C-cluster
Cys	294	299	334	Conserved in Class I/II, some III/IV
Cys	295	300	335	Ligand to FCII of C-cluster
Cys	333	338	387	Ligand to $[Fe_3S_4]$ of C-cluster
Cys	----	----	485	Ligand to E-cluster (conjecture)
Cys	----	----	488	Ligand to E-cluster (conjecture)
Cys	----	----	491	Ligand to E-cluster (conjecture)
Cys	----	----	495	Ligand to E-cluster (conjecture)
Cys	----	----	526	Ligand to F-cluster (conjecture)
Cys	----	----	529	Ligand to F-cluster (conjecture)
Cys	----	----	532	Ligand to F-cluster (conjecture)
Cys	----	----	536	Ligand to F-cluster (conjecture)
Leu	442	447	590	Restriction in tunnel (not conserved)
Cys	446	451	594	Ligand to $[Fe_3S_4]$ of C-cluster
Cys	476	481	625	Ligand to $[Fe_3S_4]$ of C-cluster
Cys	526	531	675	Ligand to Ni of C-cluster
His	----	----	680	Conserved in Class I/II
Lys	563	568	725	H-bonded to μ^2-S of C-cluster?
His	579	584	741	Conserved in most Class III/IV
His	----	----	745	Conserved in most Class I/II